# CAN THE LACK OF SYMMETRY IN THE *COBE*/DMR MAPS CONSTRAIN THE TOPOLOGY OF THE UNIVERSE?

Angélica de Oliveira-Costa[1,2], George F. Smoot[1] and

Alexei A. Starobinsky[3]

(1) Lawrence Berkeley Laboratory, Space Sciences Laboratory & Center for Particle Astrophysics, Building 50-205, University of California, Berkeley, CA 94720.

(2) Instituto Nacional de Pesquisas Espaciais (INPE), Astrophysics Division, São José dos Campos, São Paulo 12227-010, Brazil.

(3) Russian Academy of Sciences & Landau Institute for Theoretical Physics, Kosygina St. 2, Moscow 117334, Russia.

E-mails: *angelica@cosmos.lbl.gov, smoot@galaxy.lbl.gov, alstar@landau.ac.ru*

## ABSTRACT

Alhough the cubic $T^3$ "small universe" has been ruled out by *COBE*/DMR results as an interesting cosmological model, we still have the possibility of living in a universe with a more anisotropic topology such as a rectangular $T^3$ "small universe" with one or two of its dimensions significantly smaller than the present horizon (which we refer to as $T^1$- and $T^2$-models, respectively). In order to rule out these anisotropic topologies as well, we apply a new data analysis method that searches for the specific kind of symmetries that these models should produce. We find that the 2 year *COBE*/DMR data set a lower limit on the smallest cell size for $T^1$- and $T^2$-models of $3000h^{-1}$Mpc, at 95% confidence, for a scale invariant power spectrum ($n$=1). These results imply that *all* toroidal universes (cubes and rectangles) are ruled out as interesting cosmological models.

*Subject headings*: cosmic microwave background, large-scale structure of universe.

**For Reference**

**Not to be taken from this room**

# 1 Introduction

In the past few years, mainly after the discovery of CMB anisotropies by *COBE*/DMR (Smoot *et al.* 1992), the study of the topology of the universe has become an important problem for cosmologists and some hypotheses, such as the "small universe" model (see *e.g.* Ellis and Schreiber 1986), have received considerable attention. From the theoretical point of view, it is possible to have quantum creation of the universe with a multiply-connected topology (Zel'dovich and Starobinsky 1984). From the observational side, this model has been used to explain the "observed" periodicity in the distributions of quasars (Fang and Sato 1985) and galaxies (Broadhurst *et al.* 1990).

Almost all work on "small universes" has been limited to the case where the spatial sections form a rectangular basic cell with sides $L_x, L_y, L_z$ and with opposite faces topologically connected, a topology known as toroidal. The three-dimensional cubic torus $T^3$ is the simplest model among all possible multiply-connected topologies, in which all three sides have the same size $L \equiv L_x = L_y = L_z$. In spite of the fact that cubic $T^3$-model has been ruled out by *COBE* results (Sokolov 1993; Starobinsky 1993, hereafter S93; Stevens *et al.* 1993; Jing and Fang 1994; de Oliveira-Costa and Smoot 1995, hereafter dOCS95), the possibility that we live in a universe with a more anisotropic topology, such as a rectangular torus $T^3$, is an open problem that has not been ruled out yet. For instance, if the toroidal model is not a cube, but a rectangle with sides $L_x \neq L_y \neq L_z$ and with one or two of its dimensions significantly smaller than the horizon $R_H$ ($\equiv 2cH_0^{-1}$), this small

rectangular universe cannot be completely excluded by any of the previous analyses: constraints from the DMR data merely require that at least one of the sides of the cell be larger than $R_H$.

As pointed out by S93 and Fang (1993), if the rectangular $T^3$-universe has one of the cell sizes smaller than the horizon and the other two cell sizes are of the order of or larger than the horizon (for instance, $L_x \ll R_H$ and $L_y, L_z \gtrsim R_H$), the large scale CMB pattern shows the existence of a symmetry plane and if it has two cell sizes smaller than the horizon and the third cell size is of the order of or larger than the horizon (for instance, $L_x, L_y \ll R_H$ and $L_z \gtrsim R_H$), the CMB pattern shows the existence of a symmetry axis. We call the former case a $T^1$-model because the spatial topology of the universe becomes just $T^1$ in the limit $L_y, L_z \to \infty$ with $L_x$ being fixed. The later case is denoted a $T^2$-model for the same reason (the corresponding limit is $L_z \to \infty$ with $L_x, L_y$ being fixed). It is clear (and our calculations confirm it) that dependence of CMB fluctuations on any cell size is very small once it exceeds the horizon. In previous work (dOCS95), we computed the full covariance matrix for all multipole components and used a $\chi^2$-technique to place a lower limit on the cell size $L$ of the cubic $T^3$-models. However, we cannot apply this same approach to study the $T^1$- and $T^2$-universes. As we explain in the next section, the observed power spectrum of these models depends not only on the cell size but also strongly on the cell orientation relative to the Galaxy cut.

Our goal is to show that the *COBE*/DMR maps have the ability to discriminate and rule out $T^1$- and $T^2$-models. We use a different approach to

study these models in which we constrain their sizes by looking for the symmetries that they would produce in the CMB, obtaining strong constraints from the 2 year $COBE$/DMR data.

## 2 Symmetries in the CMB due to topology

If the density fluctuations are adiabatic and the Universe is spatially flat, the Sachs-Wolfe fluctuations in the CMB are given by

$$\frac{\delta T}{T}(\theta,\phi) = -\frac{1}{2}\frac{H_0^2}{c^2}\sum_{\mathbf{k}}\frac{\delta_{\mathbf{k}}}{k^2}e^{i\mathbf{k}\cdot\mathbf{r}} \tag{1}$$

(Peebles, 1982), where $\mathbf{r}$ is the vector with length $R_H \equiv 2cH_0^{-1}$ that points in the direction of observation $(\theta,\phi)$, $H_0$ is the Hubble constant (written here as $100h$ km s$^{-1}$ Mpc$^{-1}$) and $\delta_{\mathbf{k}}$ is the density fluctuation in Fourier space, with the sum taken over all wave numbers $\mathbf{k}$. Here we neglect the difference between the horizon surface and the surface of the last scattering which is justified for $l < 30$.

It is customary to expand the CMB fluctuations in spherical harmonics

$$\frac{\delta T}{T}(\theta,\phi) = \sum_{l=0}^{\infty}\sum_{m=-l}^{l} a_{lm}Y_{lm}(\hat{\mathbf{r}}), \tag{2}$$

where $a_{lm}$ are the spherical harmonic coefficients and $\hat{\mathbf{r}}$ is the unit vector in direction $\mathbf{r}$. The coefficients $a_{lm}$ are given by

$$a_{lm} = -2\pi i^l\frac{H_0^2}{c^2}\sum_{\mathbf{k}}\frac{\delta_{\mathbf{k}}}{k^2}j_l(kR_H)Y_{lm}^*(\hat{\mathbf{k}}), \tag{3}$$

where $j_l$ are spherical Bessel functions of order $l$. If we assume that the CMB fluctuations $\delta T/T$ are a Gaussian random field, the coefficients $a_{lm}$

are Gaussian random variables with zero mean and covariance matrix

$$\langle a^*_{lm} a_{l'm'} \rangle \propto \sum_{\mathrm{k}} \frac{|\delta_{\mathrm{k}}|^2}{k^4} j_l(kR_H) j_{l'}(kR_H) Y_{lm}(\hat{\mathrm{k}}) Y^*_{l'm'}(\hat{\mathrm{k}}). \tag{4}$$

In a Euclidean topology the universe is isotropic, the sum in (4) is replaced by an integral and the power spectrum $C_l$ is related to the coefficients $a_{lm}$ by

$$\langle a^*_{lm} a_{l'm'} \rangle \equiv C_l \delta_{ll'} \delta_{mm'} \tag{5}$$

(see *e.g.* Bond and Efsthatiou 1987). However, in a toroidal universe this is not the case. In this model only wave numbers that are harmonics of the cell size are allowed. We have a discrete k spectrum

$$\mathrm{k} = \frac{2\pi}{R_H} \left( \frac{p_x}{R_x}, \frac{p_y}{R_y}, \frac{p_z}{R_z} \right) \tag{6}$$

(Zel'dovich 1973; Fang and Houjun 1987), where $p_x$, $p_y$ and $p_z$ are integers and $R_x \equiv L_x/R_H$, $R_y \equiv L_y/R_H$ and $R_z \equiv L_z/R_H$.

In previous work (dOCS95), we set limits on the cubic $T^3$-models assuming that, for a given cell size, the quantity $\hat{C}_l \equiv \frac{1}{2l+1} \sum |a_{lm}|^2$ was fairly independent of the cell orientation, even with a 20° Galaxy cut. In other words, if $\hat{C}_l$ is almost independent of the cell orientation, we can make the approximation that all cell orientations for that given cell size can be simultaneously ruled out by a $\chi^2$-test on the $\hat{C}_l$ coefficients and, in that way, test our model just considering changes in the cell size $L$. However, in the case of more strongly anisotropic cell configurations such as $T^1$- and $T^2$-models, the quantity $\hat{C}_l$ does depend on the cell orientation and the $\chi^2$-test on the power spectrum cannot be used anymore. If we try to apply the power spectrum method to these models, it will require testing a six parameter family

of models with three parameters corresponding to the cell orientation in addition to the cell sizes $L_x$, $L_y$ and $L_z$.

In order to illustrate these anisotropic cell configurations, we plot a realization of two extreme cases: a $T^1$-universe (Figure 1A, upper left) with dimensions $(R_x, R_y, R_z) = (3,3,0.3)$ and a $T^2$-universe (Figure 1B, upper right) with dimensions $(R_x, R_y, R_z) = (0.3,0.3,3)$. Both models are plotted in galactic coordinates and have a scale invariant power spectrum ($n$=1). From equations (1) and (6), we see that when one of the cell sizes is smaller than the horizon ($T^1$-models), the temperatures $\delta T/T$ are almost independent of this coordinate. For instance if $R_z \ll 1$, the values of $\delta T/T$ are independent of the $z$-coordinate, *i.e.*, the values of $\delta T/T$ are symmetric about the plane formed by the $x$ and $y$-axes. This happens because of the factor $\delta_{\mathbf{k}}/k^2$ in equation (1). If we assume a power-law power spectrum with $n$=1, the r.m.s. value of this factor scales as $k^{-3/2}$, so that most of the contribution to the sum comes from small $k$-values. If $R_z \ll 1$, the term $p_z/R_z$ in equation (6) will be much greater than unity when $p_z \neq 0$, so the term with $p_z = 0$ will dominate the sum. Since this term is independent of the $z$-coordinate, the entire sum will be approximatelly independent of $z$. In the same way, if two cell sizes are smaller than the horizon ($T^2$-models), the temperatures $\delta T/T$ are aproximately independent of these coordinates. For instance if $R_x, R_y \ll 1$, the values of $\delta T/T$ are almost independent of both $x$ and $y$, *i.e.*, the values of $\delta T/T$ are almost constant along rings around the $z$-axis.

The results above remain valid for a much broader range of $n$-values

(actually, $n < 3$). Thus, the following analysis is applicable in *any* other large scale CMB experiment as well as one-degree CMB experiments. Besides, although the existence of these symmetric patterns in the large scale fluctuations $\delta T/T$ do not depend on the assumptions of gaussian statistics and absence of correlation between multipoles (see S93), we decided to use both assumptions in this analysis.

The analysis of $T^1$- and $T^2$-models is not an easy task, since there are infinitely many combinations of different cell sizes and cell orientations. In order to keep our analysis simple, we wish to adopt a statistic that is independent of cell orientation. In addition, we want a statistic that is precisely sensitive to the type of symmetries that small universes produce, so that it can rule out as many false models as possible. Finally, we would like to have a statistic that is easy to compute and that produces results that are easy to interpret. Having these criteria in mind, we choose a statistic in which we calculate the function $S(\hat{\mathbf{n}}_i)$ defined by

$$S(\hat{\mathbf{n}}_i) \equiv \frac{1}{N_{pix}} \sum_{j=1}^{N_{pix}} \frac{[\frac{\delta T}{T}(\hat{\mathbf{n}}_j) - \frac{\delta T}{T}(\hat{\mathbf{n}}_{ij})]^2}{\sigma(\hat{\mathbf{n}}_j)^2 + \sigma(\hat{\mathbf{n}}_{ij})^2}, \tag{7}$$

where $N_{pix}$ is the number of pixels that remain in the map after the Galaxy cut have taken place, $\hat{\mathbf{n}}_{ij}$ denotes the reflection of $\hat{\mathbf{n}}_j$ in the plane whose normal is $\hat{\mathbf{n}}_i$, *i.e.*,

$$\hat{\mathbf{n}}_{ij} = \hat{\mathbf{n}}_j - 2(\hat{\mathbf{n}}_i \cdot \hat{\mathbf{n}}_j)\hat{\mathbf{n}}_i \tag{8}$$

and $\sigma(\hat{\mathbf{n}}_j)$ and $\sigma(\hat{\mathbf{n}}_{ij})$ are the r.m.s. errors associated with the pixels in the directions $\hat{\mathbf{n}}_j$ and $\hat{\mathbf{n}}_{ij}$. $S(\hat{\mathbf{n}}_i)$ is a measure of how much reflection symmetry there is in the mirror plane perpendicular to $\hat{\mathbf{n}}_i$. The more perfect the

symmetry is, the smaller $S(\hat{\mathbf{n}}_i)$ will be. When we calculate $S(\hat{\mathbf{n}}_i)$ for all 6144 pixels at the positions $\hat{\mathbf{n}}_i$, we obtain a sky map that we refer to as an $S$-map. This sky map is a useful visualization tool and gives intuitive understanding of how the statistic $S(\hat{\mathbf{n}}_i)$ works.

In order to better understand $S(\hat{\mathbf{n}}_i)$, we first consider the simple model of a $T^1$-universe with $R_z \ll 1$. For this specific model, the values of $\delta T/T$ are almost independent of the $z$-coordinate, so we have almost perfect mirror symmetry about the $xy$-plane or, in spherical coordinates, $\delta T/T(\theta, \phi) \approx \delta T/T(\pi - \theta, \phi)$. When $\hat{\mathbf{n}}_i$ points in the direction of the smallest cell size (*i.e.*, $z$-direction), we have $S(\hat{\mathbf{n}}_i) \approx 1$; otherwise, $S(\hat{\mathbf{n}}_i) > 1$. An $S$-map for a $T^1$-model $(R_x, R_y, R_z) = (3,3,0.3)$ can be seen in Figure 1C (lower left). Notice in this plot that the direction in which the cell is smallest can be easily identified by two "dark spots" at $\hat{\mathbf{n}}_i \approx \hat{\mathbf{z}}$ and $\hat{\mathbf{n}}_i \approx -\hat{\mathbf{z}}$. For $T^2$-models, the only difference will be that in the place of the two "dark spots", we have a "dark ring" structure in the plane formed by the two small directions. See Figure 1D (lower right), an $S$-map of the $T^2$-model $(R_x, R_y, R_z) = (0.3,0.3,3)$.

From these two $S$-maps, we can infer two important properties: first, the direction in which the $S$-map takes its minimum value, denoted $S_o$, is the direction in which the universe is small. For a large universe such as (3,3,3), the $S_o$-directions obtained from different realizations are randomly distributed in the sky. Secondly, the distribution of $S_o$-values changes with the cell size, *i.e.*, as the universe becomes smaller, the values of $S_o$ decrease. From the definition of the $S$-map, it is easy to see that the value of $S_o$ is

independent of the cell orientation. In other words, if we rotate the cell, we will just be rotating the $S$-map, leaving its minimum value $S_o$ unchanged.

In summary, our statistic $S_o$ has all the properties that we desire: it quantifies the "smallness" of a sky map in a single number, it is independent of the cell orientation, and it is easy to work with and to interpret.

From here on, we will present our results in terms of the cell sizes $R_x$, $R_y$ and $R_z$, usually sorted as $R_x \leq R_y \leq R_z$. We remind the reader that the results are identical for all six permutations of $R_x$, $R_y$ and $R_z$.

## 3 Data analysis

We rewrite the exponential in equation (1) as

$$e^{i\mathbf{k}\cdot\mathbf{r}} = \cos\mathbf{k}\cdot\mathbf{r} + i\sin\mathbf{k}\cdot\mathbf{r} = \cos(2\pi\gamma) + i\sin(2\pi\gamma), \tag{9}$$

where $\mathbf{k}$ is given by (6), $\mathbf{r}$ is the vector with lenght $R_H \equiv 2cH_0^{-1}$ and $\gamma = \left(\frac{p_x}{R_x}x + \frac{p_y}{R_y}y + \frac{p_z}{R_z}z\right)$. If the density fluctuation in Fourier space $\delta_\mathbf{k}$ has random phases, we have $\delta_\mathbf{k} = N(g_1 + ig_2)$, so that $\langle|\delta_\mathbf{k}|^2\rangle = \langle|g_1+ig_2|^2N^2\rangle = 2N^2$, where $N$ is a constant and $g_1$ and $g_2$ are two independent Gaussian random variables with zero mean and unit variance. Assuming a power law power spectrum with shape $P(k) \equiv \langle|\delta_\mathbf{k}|^2\rangle = Ak^n$, where $A$ is the amplitude of scalar perturbations and $n$ the spectral index, we have $N = \sqrt{\frac{A}{2}}k^{n/2}$, so that the term $\delta_\mathbf{k}/k^2$ in (1) is given by

$$\frac{\delta_\mathbf{k}}{k^2} \propto \alpha^{\frac{n-4}{4}}, \tag{10}$$

where $\alpha \equiv \left(\frac{p_x}{R_x}\right)^2 + \left(\frac{p_y}{R_y}\right)^2 + \left(\frac{p_z}{R_z}\right)^2 \propto k^2$. Substituting (9) and (10) in (1), we can construct simulated skies by calculating

$$\frac{\delta T}{T}(\theta,\phi) \propto \sum_{p_x,p_y,p_z} [g_1 \cos(2\pi\gamma) - g_2 \sin(2\pi\gamma)] \alpha^{\frac{n-4}{4}}. \qquad (11)$$

Since the cubic $T^3$ case has already been ruled out as an interesting cosmological model (see *e.g.* dOCS95), we restrict our analysis here to the $T^1$ and $T^2$ cases for $n$=1. This is a two parameter family of models specified by $R_x$ and $R_y$, with $R_z = \infty$. For numerical convenience, we set $R_z$=3 instead, as this is found to give virtually the same results as $R_z = \infty$. We adopt $n$=1, as we found that "small universe" models with different $n$-values are even more inconsistent with the observed data.

The large scale fluctuations observed on the celestial sphere by a CMB experiment can be modeled as being the fluctuations given in (11) multiplied by an experimental beam function

$$e^{-(R_H \theta k_\perp)^2/2}, \qquad (12)$$

where $k_\perp$ is the length of the k-component perpendicular to the line of sight and $\theta$ is the width of the Gaussian beam given by $\theta$ = FWHM/$2\sqrt{\ln 2} \approx$ 0.6 FWHM, where FWHM is the full width of the beam at its half maximum. We make the approximation that the sky area covered by the beam is flat (this is equivalent to smoothing in the plane perpendicular to the line of sight $\hat{\mathbf{r}}$). Since $k_\perp \equiv |\hat{\mathbf{r}} \times \hat{\mathbf{k}}|$, we have that $k_\perp^2 = k^2 - (\hat{\mathbf{r}} \cdot \hat{\mathbf{k}})^2$. We use FWHM = 7° in our simulations, which is the FWHM of the $COBE$/DMR beam.

In the real sky map, we do not have all sky coverage. Because of the uncertainty in Galaxy emission, we are forced to remove all pixels 20° below

and above the Galaxy plane, which represents a loss of almost 34% of all pixels. However, performing Monte Carlo simulations with and without the Galaxy cut, we find that the Galaxy cut does not change the final distribution of $S_0$ much. Due to the smaller data sample, the Galaxy cut weakens the lower limit on the cell size slightly.

We model the noise $n_i$ at each pixel $i$ as independent Gaussian random variables with mean $\langle n_i \rangle$ =0 and variance $\langle n_i n_j \rangle = \sigma_{ij}\delta_{ij}$ (Lineweaver *et al.* 1994), and add it to the temperature values given by (11). The level of noise in the DMR maps is a source of serious concern in our analysis: high levels of noise can make it impossible to discriminate the different topological models. In order to reduce the noise and increase the signal-to-noise ratio in the simulated skies and real data, we smooth both once more by 7° before calculating $S$-map, which corresponds to a total smearing of $\sqrt{(7°)^2 + (7°)^2} \approx 10°$.

We generate our simulated skies as standard DMR maps with 6144 pixels for $n$=1, with a Galaxy cut of 20°, FWHM = 7°, the monopole and dipole removed, add noise and normalize to $\sigma_{7°} = 38.6\mu$K (the r.m.s. value at 7° extracted from our DMR map, a 2-year combined 53 plus 90 GHz map with monopole and dipole removed). Fixing a cell size, we construct a simulated sky according to (11), we smooth this once more by 7° and use the statistic defined in (7) to obtain an $S$-map from which we extract its minimum value $S_0$. Repeating this procedure 300 times, we obtain the probability distribution of $S_0$ for that fixed cell size. When we repeat this same procedure for different cell sizes, we are able to construct Figure 2.

In Figure 2A (left), we show the cumulative probability distribution of $S_o$ obtained from the Monte Carlo simulations for the cell sizes $(R_x, R_y, R_z)$ = (0.5,0.5,3), (0.6,0.6,3), (0.7,0.7,3) and (3,3,3). The horizontal lines indicate the confidence levels of 95%, 90% and 68% (from top to bottom). Comparing these curves with the value $S_o^{DMR} = 1.85$ (represented in the plot by the vertical straight line), where $S_o^{DMR}$ is the $S_o$ value extracted from our data set, we conclude that $T^2$-models with smallest cell sizes $R_x, R_y \lesssim 0.5$ can be ruled out at 95% confidence. As the second cell size $R_y$ is increased, the curves shift to the left of the $T^2$-models and we can rule out $T^1$-models for $R_x \lesssim 0.5$ at a similar confidence level, see Figure 2B (right). In this plot, we show the cumulative probability distribution of $S_o$ obtained from Monte Carlo simulations for the cell sizes $(R_x, R_y, R_z)$ = (0.5,3,3), (0.6,3,3), (0.7,3,3) and (3,3,3). A more complete picture of the cell size limits is obtained when we construct a two-dimensional grid for different values of the cell sizes $(R_x, R_y, R_z)$ with $R_z = 3.0$ and $0.2 < R_x, R_y < 3.0$ (see Figure 3). The thin-shaded, thick-shaded and grey regions correspond, respectively, to the models ruled out at 68%, 90% and 95% confidence. Notice in this plot that all contours are almost $L$-shaped, which means that, to a good approximation, the level in which a model $(R_x, R_y)$ is ruled out depends only on the *smallest* cell size, $R_{min} \equiv \{R_x, R_y\}$. We see that $R_{min} \gtrsim 0.5$ at 95% confidence.

# 4 Conclusions

We have shown that the $COBE$/DMR maps have the ability to discriminate and rule out $T^1$ and $T^2$ topological models. We have presented a new statistic to study these anisotropic models which quantifies the "smallness" of a sky map in a single number, $S_o$, which is independent of the cell orientation, is easy to work with and is easy to interpret.

From the $COBE$/DMR data, we obtain a lower limit for $T^1$- and $T^2$-models of $R_x \gtrsim 0.5$, which corresponds to a cell size with smallest dimension of $L=3000h^{-1}$Mpc. This limit is at 95% confidence and assumes $n=1$. Since the topology is interesting only if the cell size is considerably smaller than the horizon, so that it can (at least in principle) be directly observed, these models lose most of their appeal. Since the cubic $T^3$ case has already been ruled out as an interesting cosmological model (see *e.g.* dOCS95), and $T^1$- and $T^2$-models for small cell sizes are ruled out, this means that *all* toroidal models (cubes and rectangles) are ruled out as interesting cosmological models.

We would like to thank Jon Aymon and Al Kogut for the help with the *COBE* library subroutines and Douglas Scott, Daniel Stevens and Max Tegmark for many useful comments and help with the manuscript. AC acknowledges SCT-PR/CNPq Conselho Nacional de Desenvolvimento Científico e Tecnológico for her financial support under process No. 201330/93-8(NV). AS was supported in part by the Russian Foundation for Basic Research, under grant No. 93-02-3631, and by the Russian Research Project "Cosmomicrophysics". AC and AS were also supported in part by the National Science Foundation, under grant No. PHY94-07194, during their visit to ITP, USCB and participation in the Conference on CMB Fluctuations (Santa Barbara, 22-24 February 1995) where this project was begun. This work was also supported in part by the Director, Office of Energy Research, Office of High Energy and Nuclear Physics, Division of High Energy Physics of the U.S. Department of Energy under contract No. DE-AC03-76SF00098.

## References


Bond, J.R. & Efsthatiou, G.P. 1987, MNRA, 226, 655.

Broadhurst, T.J., Ellis, R.S., Koo, D.C. & Szalay, A.S. 1990, Nature, 343,726.

de Oliveira-Costa, A. & Smoot, G.F. 1995, ApJ, 448, 447 ("dOCS95").

Ellis, G.F.R. & Schreiber, G. 1986, Phys. Lett. A, 115, 97.

Fang, L.Z. 1993, Mod. Phys. Lett. A, 8, 2615.

Fang, L.Z. & Houjun, M. 1987, Mod. Phys. Lett. A, 2, 229.

Fang, L.Z. & Sato, H. 1985, Gen. Rel. and Grav., 17, 1117.

Jing, Y.P. & Fang, L.Z. 1994, Phys. Rev. Lett., 73, 1882.

Lineweaver, C. et al. 1994, ApJ, 436, 452.

Peebles, P.J.E. 1982, ApJ, 263, L1.

Smoot, G.F. et al. 1992, ApJ, 396, L1.

Sokolov, I.Y. 1993, JETP Lett., 57, 617.

Starobinsky, A.A. 1993, JETP Lett., 57, 622 ("S93").

Stevens, D., Scott, D. & Silk, J. 1993, Phys. Rev. Lett., 71, 20.

Zel'dovich, Ya B. 1973, Comm. Astrophys. Space Sci., 5, 169.

Zel'dovich, Ya B. & Starobinsky, A.A. 1984, Sov. Astron. Lett., 10, 135.

## Figure Captions:

Figure 1: Simulated sky maps for the $T^1$- and $T^2$-models and their $S$-maps. (A) $T^1$-model with dimensions $(R_x, R_y, R_z)$ = (3,3,0.3); (B) $T^2$-model with dimensions $(R_x, R_y, R_z)$ = (0.3,0.3,3); (C) $S$-map of the $T^1$-model shown in $(A)$; (D) $S$-map of the $T^2$-model shown in $(B)$.

Figure 2: Cumulative probability distribution of $S_\circ$ for $T^1$- and $T^2$-models obtained from Monte Carlo simulations. (A) Simulations for $T^2$-universes with dimensions $(R_x, R_y, R_z)$ = (0.5,0.5,3) or dot-dashed line, (0.6,0.6,3) or dashed line, and (0.7,0.7,3) or dotted line. (B) Simulations for $T^1$-universes with dimensions $(R_x, R_y, R_z)$ = (0.5,3,3) or dot-dashed line, (0.6,3,3) or dashed line, and (0.7,3,3) or dotted line. In both pictures the model $(R_x, R_y, R_z)$ = (3,3,3) is represented by a solid line, $S_\circ^{DMR} = 1.85$ (vertical straight line) and the horizontal solid lines indicate the confidence levels of 95%, 90% and 68% (from top to bottom).

Figure 3: Grid of cumulative probability distributions of $S_\circ$ for $T^1$- and $T^2$-models obtained from Monte Carlo simulations. The thin-shaded, thick-shaded and grey regions correspond, respectively, to the models ruled out at 68%, 90% and 95% confidence.

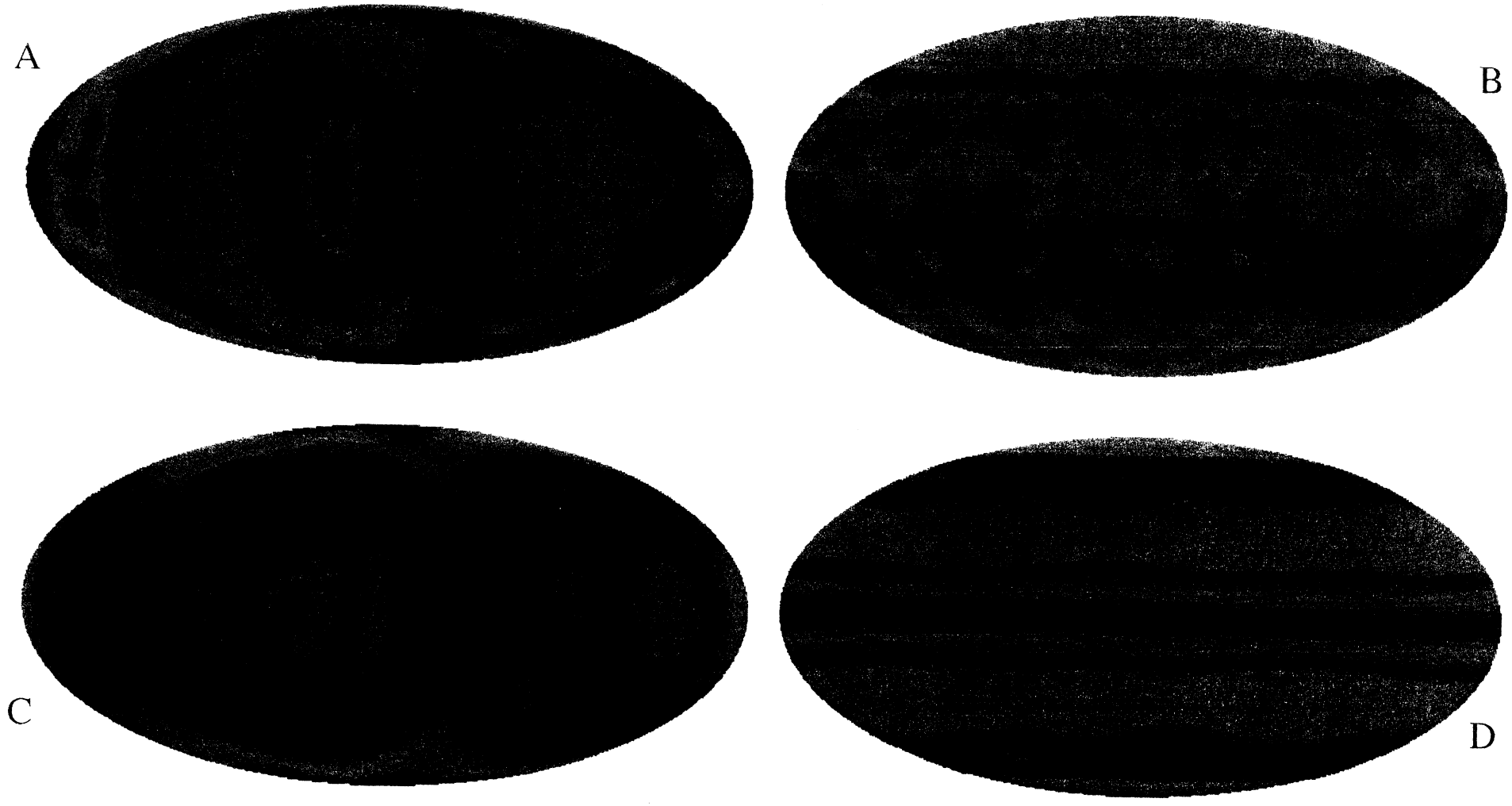


de Oliveira-Costa, Smoot & Starobinsky 1996

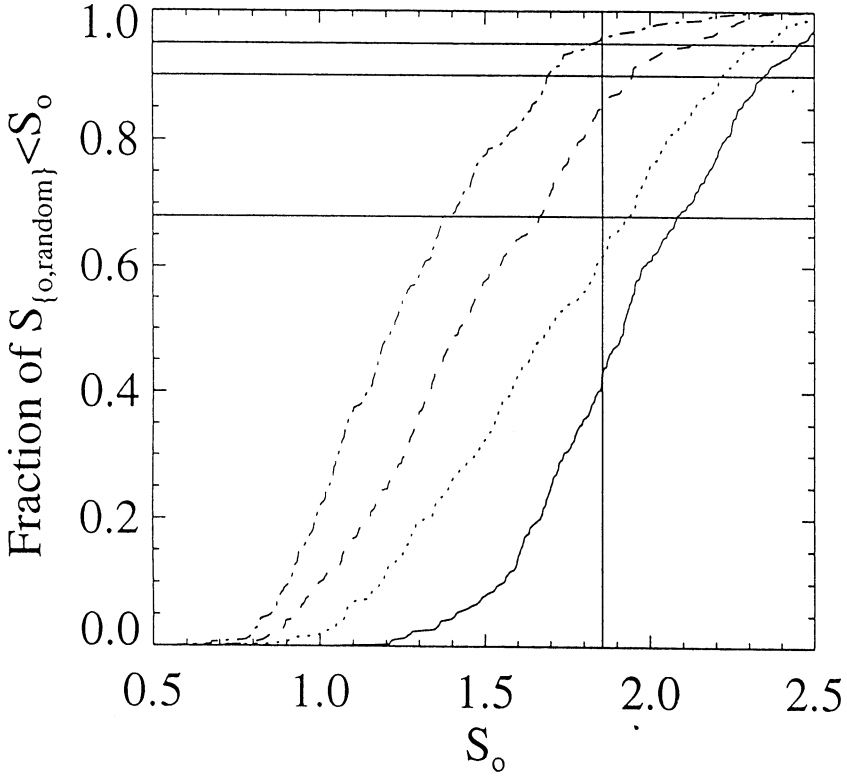
Fraction of $S_{\{o,random\}}<S_o$
1.0
0.8
0.6
0.4
0.2
0.0
0.5
1.0
1.5
2.0
2.5
$S_o$

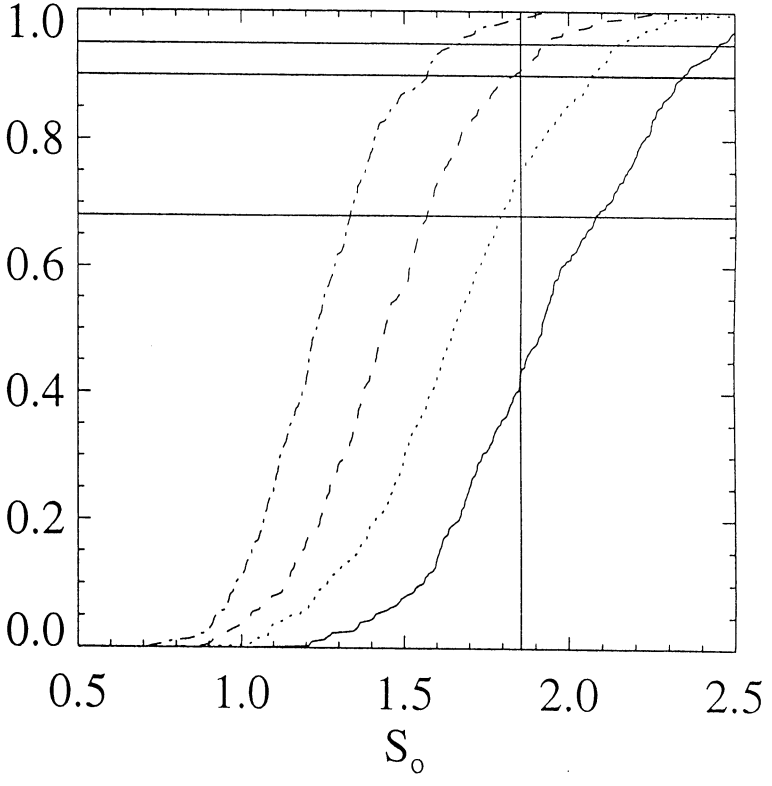
1.0
0.8
0.6
0.4
0.2
0.0
0.5
1.0
1.5
2.0
2.5
$S_o$

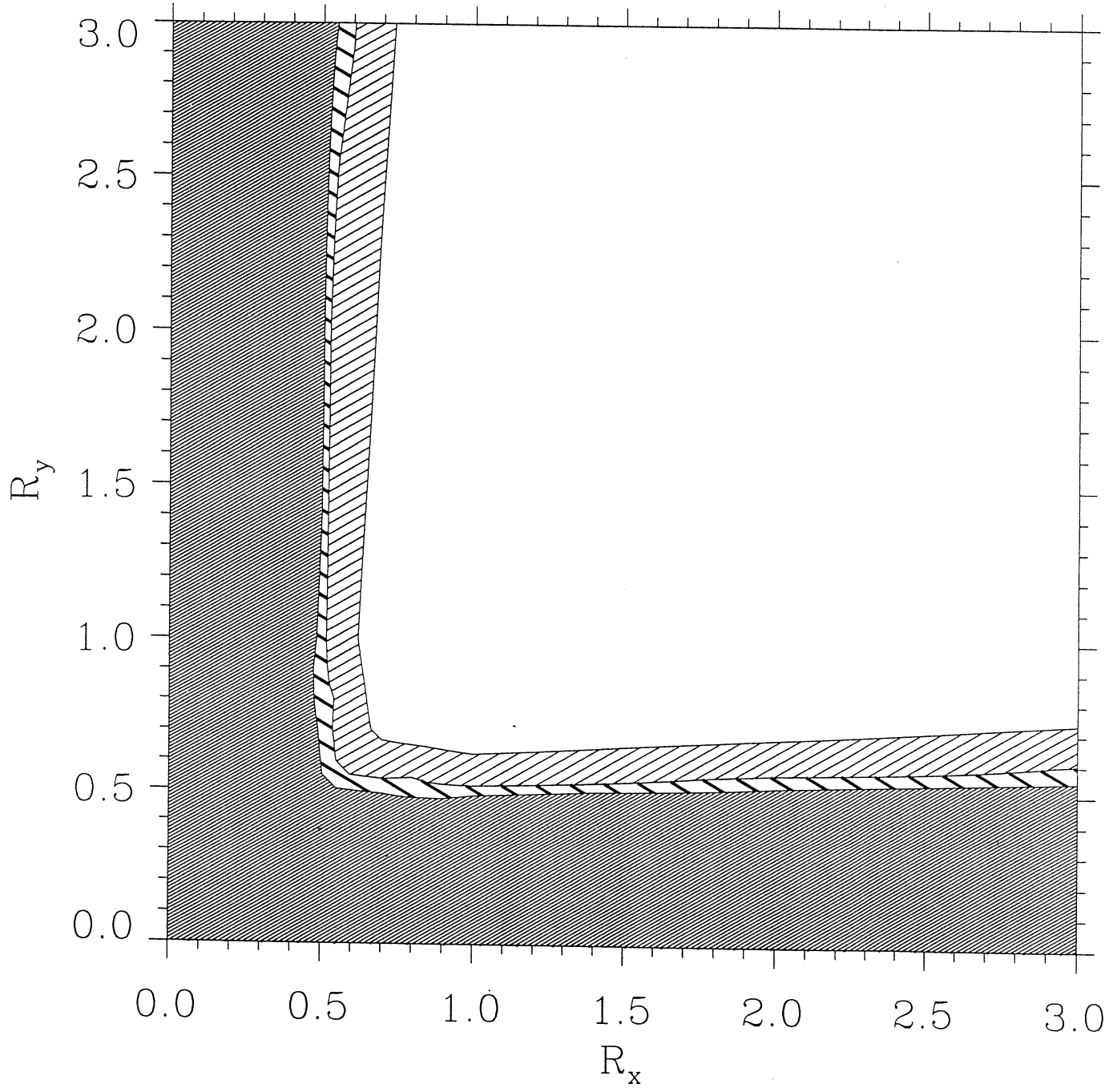
3.0
2.5
2.0
1.5
1.0
0.5
0.0
$R_y$
0.0
0.5
1.0
1.5
2.0
2.5
3.0
$R_x$